PUBLIC SUBMISSION

As of: December 29, 2011
Received: December 19, 2011
Status: Pending_Post
Tracking No. 80f85a98
Comments Due: December 19, 2011
Submission Type: Web

Docket: NRC-2011-0259
Draft Environmental Assessment and Draft Finding of No Significant Impact

Comment On: NRC-2011-0259-0001
Florida Power & Light Company, Turkey Point, Units 3 and 4; Draft Environmental Assessment and Draft Finding of No Significant Impact Related to the Proposed License Amendment to Increase the Maximum Reactor Power Level

76 FR 71379
11/17/2011 (1)

Document: NRC-2011-0259-DRAFT-0001
Comment on FR Doc # 2011-29718

Submitter Information

Name: Ed Swakon
Submitter's Representative: Ed Swakon
Organization: EAS Engineering

General Comment

Please add the attached to the public record for this project.

Attachments

Final Letter to NRC - 12-12-2011-As sent

SUNSI Review Complete
Template = ADM-013

E-RIDS = ADM-03
Add = J. Paige (JCP4)

Atlantic Civil, Inc.
9350 South Dixie Highway ▪ Suite 1250 ▪ Miami, FL 33156 ▪ 305-670-9610 ▪ Fax: 305-670-6787

STEVE TORCISE, JR.
President
Chief Executive Officer

December 12, 2011

Mr. Jason C. Paige
Plant Licensing Branch 11-2
Division of Operating Reactor Licensing
Office of Nuclear Reactor Regulation
U.S. Nuclear Regulatory Commission
Washington, D.C. 20555-0001

Re: Proposed Turkey Point Power Plant Uprate Units 3 and 4 (ME4907 and ME4908)
Draft Environmental Assessment and Finding of No Significant Impact

Dear Mr. Paige:

Thank you for the opportunity to comment on the Draft Environmental Assessment and Finding of No Significant Impact for Florida Power and Light's (FPL) proposed Turkey Point Power Plant's uprating for Units 3 and 4. While we are generally supportive of FPL's proposed uprating, we have taken the opportunity to review the draft Finding of No Significant Impact (FONSI) and wanted to share our concern about the reported findings. Our concern is based upon the direct and express conflict between the FONSI on the one hand and 28 years of monitoring data on the other. Our concern arises from our experience and ownership of adjacent property. Figure 1 shows the relationship between the Turkey Point Power plant and our property. This figure also shows the existing farming areas and the locations of the major wellfields in the area.

The fundamental problem is that the Cooling Canal System (CCS) and interceptor ditch system do not perform as originally intended. This is a clear factual conclusion supported by 28 years of corroborating data. While the concept of the cooling system is theoretically sound, over time, because the majority of the makeup water is saline, drawn in from Biscayne Bay through the porous aquifer, evaporation creates hyper-saline water in the CCS. This hyper-saline water is not adequately contained by the hydraulic gradient created with the interceptor ditch along the west side of the CCS. As a result, the CCS is creating a significant adverse environmental impact on the groundwater. This impact extends well beyond the footprint of the CCS.

The hyper-saline water below the CCS comprises a dense plume that extends miles beyond the footprint in all directions. The fact that salinity values beyond the CCS footprint are higher than background values of Biscayne Bay is clear and compelling evidence that the hyper-saline water from the CCS is not being contained. FPL's NPDES permit does not authorize offsite discharges and the existing agreement between FPL and the SFWMD dating back to 1972 (and modified 5 times, with the most recent in 2009) commands that:

> *"... the purpose of the system is to restrict the movement of saline water from the cooling water system westward of the Levee 31E adjacent to the cooling water system to those amounts which would occur without the existence of the cooling canal system."*

These supplemental agreements were **conditions precedent** to the issuance of regulatory permits that allowed FPL to construct Turkey Point and continue its operations. These historical and persistent impacts have been acknowledged by various regulatory agencies including Florida Department of Environmental Protection (FDEP), the South Florida Water Management District (SFWMD) and Miami-Dade County.

Preliminary studies by SFWMD and the United States Geological Survey (USGS) (Hughes et al, 2009) of the saltwater plume surrounding FPL CCS strongly suggest that it has caused a leading saline edge to migrate far enough west to pose health risks for drinking water wells for the Florida Keys and Homestead, Florida residents. This hyper-saline intrusion also threatens the Everglades restoration projects intended to revive historic freshwater flows to Biscayne Bay.

ACI engaged professionals to develop groundwater/saltwater intrusion models covering a large geographic area of south Miami Dade County, including the CCS area. The models conclude that the CCS has caused saltwater intrusion to extend well beyond the interceptor ditch boundary and much farther westward than the intrusion would have been without the hyper-saline CCS. Data collected by FPL itself, pursuant to several agreements between it and SFWMD, supports that conclusion. Data collected by FPL within the last year clearly documents the problem. On this point, Figures 2 & 3 show data for two parameters, chloride and tritium, collected by FPL within the last year. This data clearly shows that water from the CCS has migrated well beyond the footprint of the CCS.

The Generic Environmental Impact Statement for the License Renewal of Nuclear Plants – Supplement 5 – Regarding Turkey Point Units 3 and 4 – Final Report published ten years ago in the Federal Register dated January 2002, (GEIS-2002) was the last environmental assessment conducted of Turkey Point. The GEIS-2002 incorrectly asserted that the CCS was a closed system with an interceptor ditch along the CCS's west side that ".... prevents flow of hyper-saline water from the cooling canals toward the Everglades." i.e. west (Page 2-7 of GEIS-2002). A decade later, this 2011 Draft Environmental Assessment (DEA) ignores hundreds of data

points from numerous monitoring wells that clearly demonstrate that the interceptor ditch does not prevent (and has not prevented) the hyper-saline water from migrating westward.

The DEA will allow, intentionally or unintentionally, significant adverse environmental impacts to Biscayne Bay, the Biscayne Aquifer and the Everglades that will continue ungoverned if the past monitoring results remain ignored. The proposed uprate will further increase the salinity in the CCS. Predictably, the cooling waters will become even more hyper-saline, thus threatening the adjacent freshwater bodies, as evidenced by the monitoring data collected during the last 28 years. This saltwater intrusion into the freshwater bodies threatens the purposes for which those freshwater systems serve and amounts to continuing and significant Clean Water Act violations.

The following DEA conclusions raise specific concerns:

Page 11

"The field data collected prior to implementation of the proposed EPU will be used to characterize existing environmental conditions from current PTN operations. The CoC allows the FDEP to require additional measures if the pre- and post-EPU monitoring data are insufficient to evaluate changes as a result of the EPU. If the data indicate an adverse impact, additional measures, including enhanced monitoring, modeling or mitigation, would likely be required to evaluate or to abate such impacts."

This statement suggests that the existing monitoring data does not show an adverse impact. EAS Engineering, however, using FPL's own historical monitoring data, has shown that contaminants from the CCS (chlorides, sulfates and tritium in particular) have travelled a mile or more to the west of the interceptor ditch, resulting in violations of G-II ground water standards in this area (See the attached figures), which is the boundary of the no discharge NPDES permit.

Furthermore, this statement suggests that additional measures would likely be required to abate such impacts. As of yet the FDEP has not acted on the data presented. The existing evidence is compelling that the CCS in not functioning properly and agencies, including the SFWMD, FDEP and the NRC, must act now to prevent further damage.

Page 12

"Approving the proposed EPU license amendment is not expected to cause significant impacts greater than current operations because the monitoring plan will provide data for FPL and state agencies to assess the effectiveness of current environmental controls and additional limits and controls could be imposed if the impacts are larger than expected. Therefore, there would be no significant impact to the groundwater following implementation of the proposed EPU."

There is no basis for this statement. Continued monitoring, when more than 28 years of data documenting a problem exists, is not a basis for a finding no significant impact. The existing data already shows that water quality violations attributable to the CCS are occurring. In fact, the

additional monitoring included in the 5th supplement to the original 1972 agreement between FPL and the SFWMD documents the problem even more clearly. See figures 2 & 3.

Substantial and meaningful intervention and mitigation are needed now to correct the existing problem of CCS water migrating westward through the groundwater. This Draft Environmental Assessment must mandate a solution to the impacts being caused by the CCS today and the increased impacts that will result from the uprate. The significance of the water quality violation is great enough that a "monitoring only" requirement is not an acceptable solution and FONSI is not acceptable.

Page 14

"Because the cooling canal system is unconnected to Biscayne Bay, Card Sound, or any natural water body, changes to the conditions within the cooling canal system would not affect any aquatic species' populations in the natural aquatic habitats. Therefore, the staff concludes that there would be no significant impacts to aquatic resources as a result of the proposed EPU."

On page 8, however, the following statement is made:

"Because the PTN canals are unlined, it is likely that there is an exchange of water between the PTN canal system and local groundwater and Biscayne Bay."

These two statements are contradictory. There is an exchange of water between the CCS and local groundwater and Biscayne Bay, so changed conditions in the CCS could certainly affect aquatic species populations in Biscayne Bay and in local canals.

Page 17

"Potential socioeconomic impacts from the proposed EPU include increased demand for short-term housing, public services, and increased traffic in the region due to the temporary increase in the number of workers at the PTN site required to implement the EPU. The proposed EPU could also increase tax payments due to increased power generation."

There is no discussion of adverse economic impacts to nearby property owners whose property values and development rights are adversely affected by the westward migration of the salt front that is caused by high salinity water generated in the CCS. We have been forced to install and monitor over 25 monitoring wells and to demonstrate that the salt front had not reached our quarries yet. We have also had depth restrictions placed on our quarry excavations because of the potential for saltwater intrusion. These restrictions and monitoring are expensive and time-consuming and would not have been imposed if the westward movement of the salt front had been halted by the interceptor ditch, as required.

Likewise, there is no discussion of the potential impact to citizens in south Miami-Dade County and Monroe County who rely on well water pumped from the Biscayne Aquifer. If salt intruded ground water reaches their wells, they will be forced to pay for expensive alternative

water sources. The Florida Keyes wellfield and the wellfield supplying Turkey Point, the Newton Wellfield are at risk.

The economy in the South Miami Dade County area is heavily dependent on farming. Not only is a significant portion of our land farmed, as shown on Figure 1 there are many other large farms in the area. All of these farmed areas rely upon groundwater for irrigation that is also potentially impacted by the continued salt front migration.

The NRC in this Draft Environmental Assessment must address and require prompt solutions to the problems being caused by the CCS.

Summary

To summarize, our concerns with this proposed EA are:

1. FPL claims that the cooling canal is a closed system, but obviously it is not. FPL's monitoring data shows that the unlined cooling canal system exchanges water with adjacent ground water. FDEP designated the groundwater within the cooling canal system as G-III waters (non-potable aquifer not subject to compliance with groundwater standards) and the NPDES Permit only authorized a discharge to those G-III waters. FPL's groundwater monitoring data shows that contaminants from the cooling canals have migrated west of L-31E and the interceptor ditch into G-II waters (See the attached figures).

2. In anticipation of directly causing saltwater intrusion, the interceptor ditch was intended "*...to restrict movement of saline water from the cooling water system westward of Levee 31E adjacent to the cooling water system to those amounts which would occur without the existence of the cooling canal system.*" (SFWMD, 1983). The interceptor ditch has not been effective and has not contained the hypersaline water of the cooling canal system. FPL's monitoring data confirms this (See the attached figures 2 & 3). These figures show the chloride and tritium data collected by FPL in December 2010 and February 2011 respectively as an overlay on Figure 1. This indicates water quality violations and warrants remedial action by FPL to correct the problem before the uprate is initiated.

3. FPL has not acknowledged, controlled or adequately addressed the existing water quality violation. The proposed uprate will increase the salinity in the cooling canal system, which will exacerbate the existing water quality violation.

4. Because of this unaddressed water quality violation, other property owners have had to go to extraordinary efforts and costs to prove that saltwater intrusion has not reached their property. The NPDES permit did not authorize any injury to the public or private property or any invasion of personal rights, nor authorize infringements of federal, state or local laws or

regulations. The rights of nearby property owners clearly have been violated by the cooling system's influence on saltwater intrusion.

5. Until FPL addresses the existing water quality violations, the facility should not be allowed to increase its output and there should not be a Finding of No Significant Impact for the proposed uprate without mitigating the existing significant adverse impacts of the CCS. This Draft Environmental Assessment must mandate a solution to the impacts being cause by the CSS today and the increased impacts that will result from the uprate.

We remain willing to meet with Florida Power and Light and stakeholders to collaborate on reasonable and effective solutions which will enable FPL to proceed with its proposed project while protecting the interests of the community which surrounds Turkey Point's operations. If you have any questions or need additional information, please feel free to call us.

Sincerely,

Atlantic Civil Inc.

Steve Torcise, Jr.
President
spl
encl

cc: Steve Torcise
Steve Walker
Edward A. Swakon

9802.760.docx

REFERENCES

Hughes, J.D., C.D. Langevin & L. Brakefield-Goswami. 2009. Effect of hypersaline cooling canals on aquifer salinization. Hydrogeology Journal, 12 August 2009. DOI 10.1007/s10040-009-0502-7.

SFWMD. 1983. Fourth Supplemental Agreement with FPL, July 15, 1983.

SFWMD. 2009. Fifth Supplemental Agreement with FPL.

U.S. Nuclear Regulatory Commission. 2002. Generic Environmental Impact Statement for License Renewal of Nuclear Plants, Supplement 5, Regarding Turkey Point Units 3 and 4, Final Report. NUREG-1437 Supplement 5.

FPL Monitoring Stations
Location Map

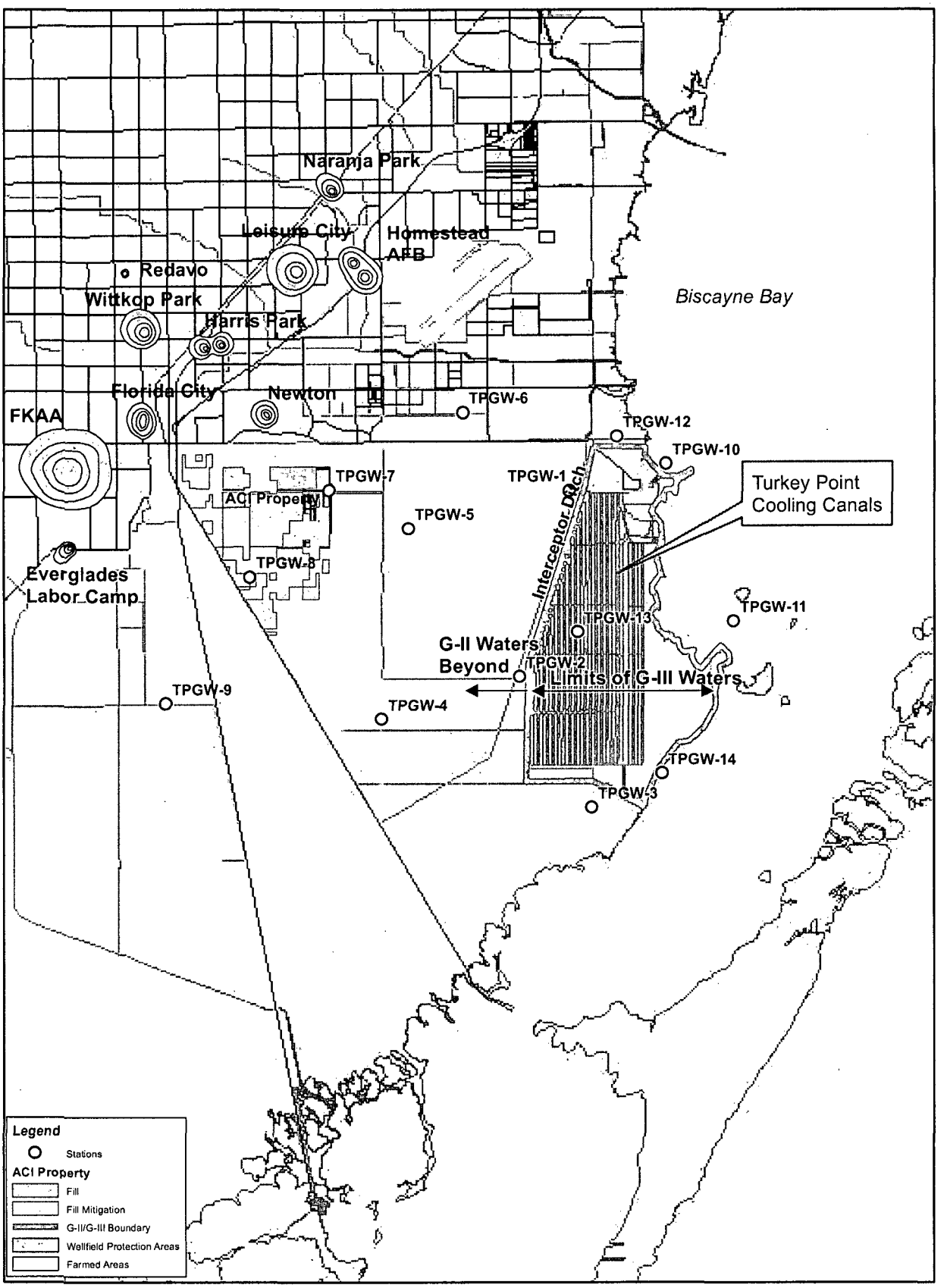

NRC Exhibit_Fig 1.pdf

EAS Engineering, Inc.

FPL Monitoring Stations
Deep Chloride - December, 2010

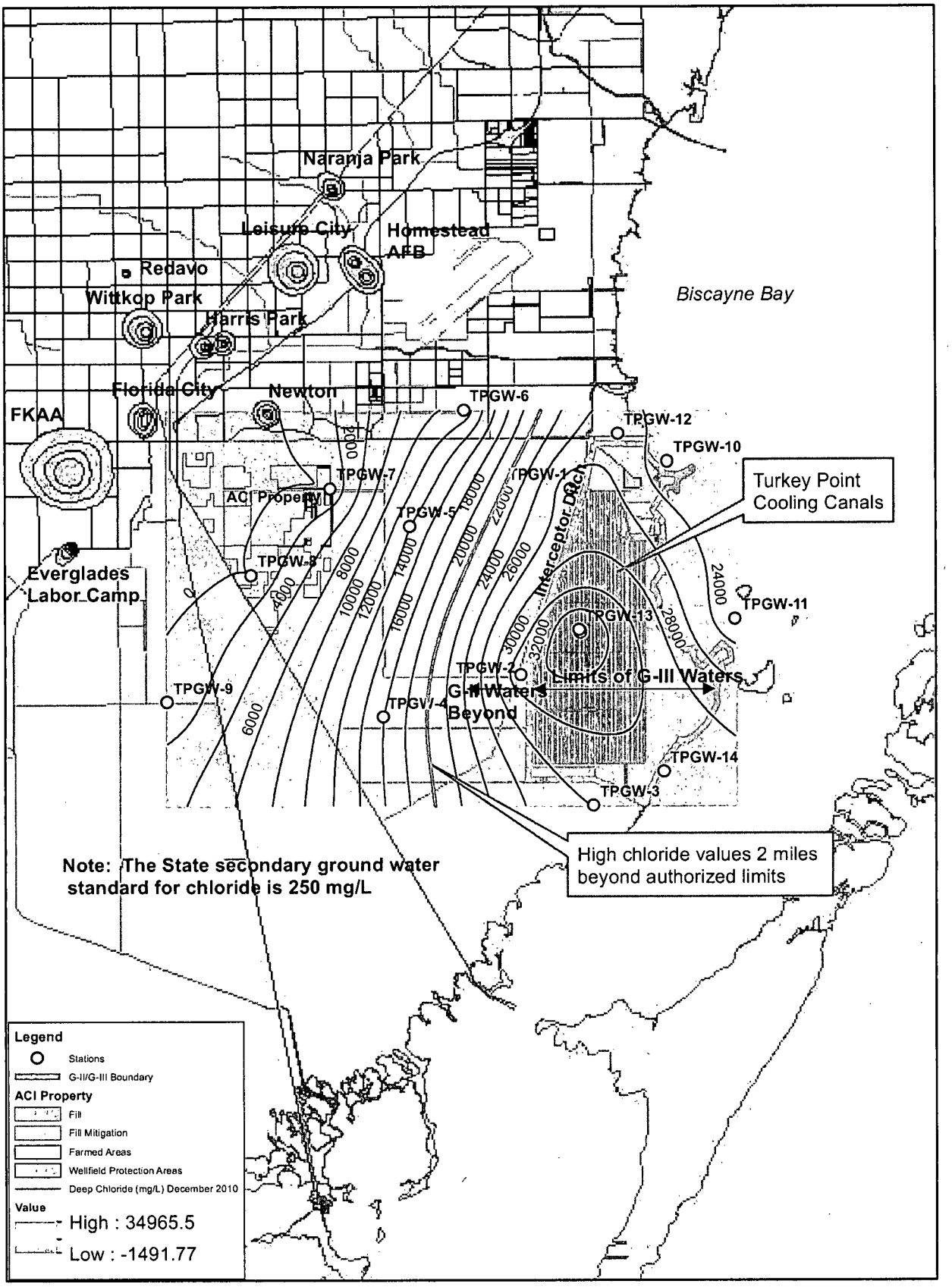

NRC Exhibit_FPL_Chloride_Dec-10_Deep.pdf

EAS Engineering, Inc.

FPL Monitoring Stations
Deep Tritium - February, 2011

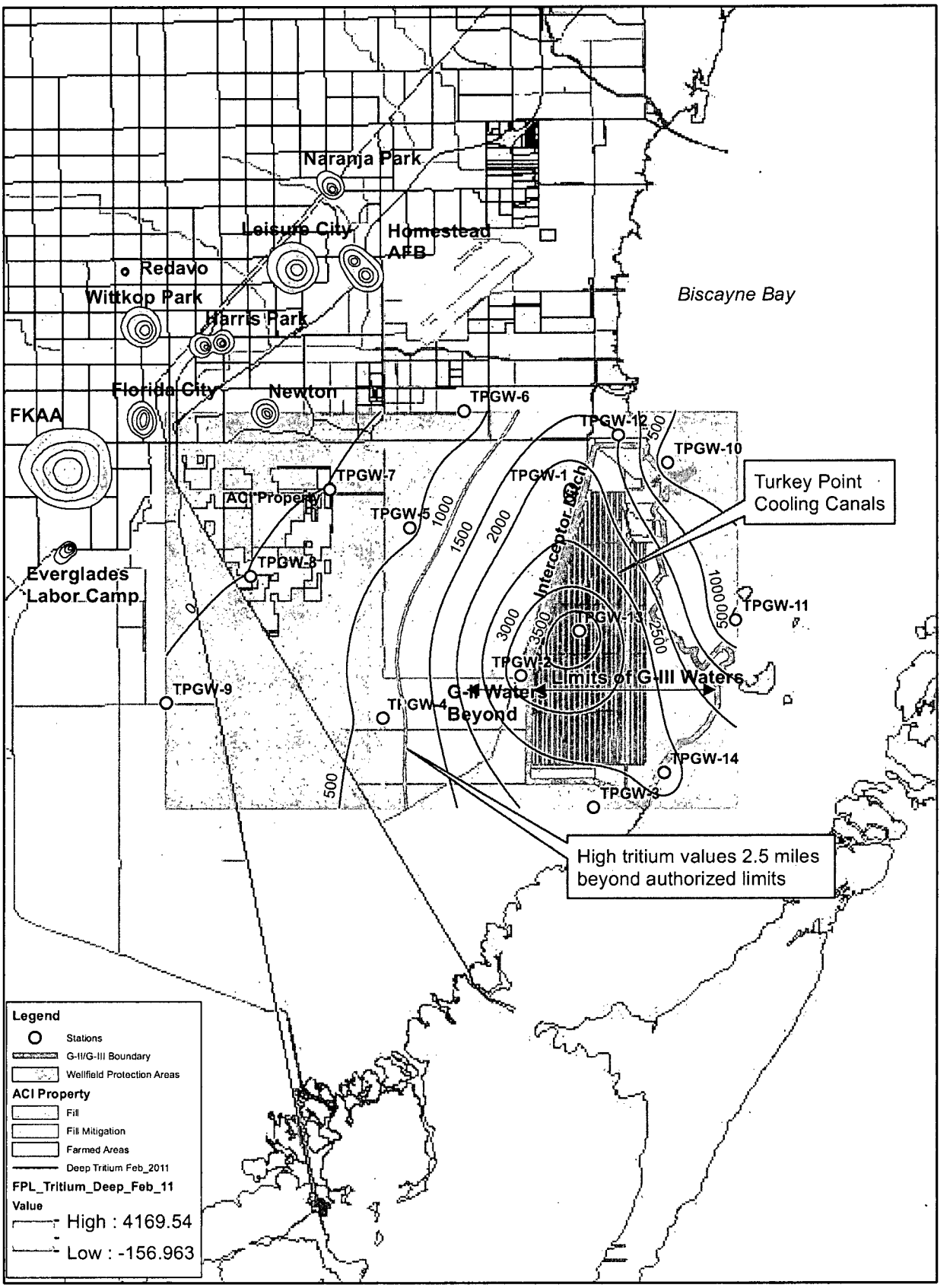

NRC Exhibit_FPL_Tritium_Feb-11_Deep.pdf

EAS Engineering, Inc.

Effect of hypersaline cooling canals on aquifer salinization

Joseph D. Hughes · Christian D. Langevin · Linzy Brakefield-Goswami

Abstract The combined effect of salinity and temperature on density-driven convection was evaluated in this study for a large ($28km^2$) cooling canal system (CCS) at a thermoelectric power plant in south Florida, USA. A two-dimensional cross-section model was used to evaluate the effects of hydraulic heterogeneities, cooling canal salinity, heat transport, and cooling canal geometry on aquifer salinization and movement of the freshwater/saltwater interface. Four different hydraulic conductivity configurations, with values ranging over several orders of magnitude, were evaluated with the model. For all of the conditions evaluated, aquifer salinization was initiated by the formation of dense, hypersaline fingers that descended downward to the bottom of the 30-m thick aquifer. Saline fingers reached the aquifer bottom in times ranging from a few days to approximately 5 years for the lowest hydraulic conductivity case. Aquifer salinization continued after saline fingers reached the aquifer bottom and coalesced by lateral movement away from the site. Model results showed that aquifer salinization was most sensitive to aquifer heterogeneity, but was also sensitive to CCS salinity, temperature, and configuration.

Keywords Coastal aquifers · Thermal conditions · Groundwater density/viscosity · Salt-water/fresh-water relations · USA

Introduction

Saline lakes, salt pans, playas, sabkhas, salinas, and salt flats develop in arid and semiarid environments throughout the world where evaporation exceeds precipitation (Yechieli and Wood 2002). There is a potential for complex groundwater flow beneath these saline features because of unstable density stratification caused by higher density groundwater overlying lower density groundwater. Unstable density configurations can occur in many other natural settings such as along permeable zones where freshwater is in contact with saline layers, and around salt domes (Schincariol and Schwartz 1990). Unstable density-driven finger convection, a process which can augment mass transfer rates and expand the spatial extent of dissolved solutes, is a more effective transport mechanism than its stable counterpart (Nield et al. 2008). For this reason, density-driven free convection has been used to explain rapid salinization of coastal aquifers (Post and Kooi 2003).

Although natural saline systems are areally extensive (Yechieli and Wood 2002), engineered water-management systems can create comparable potential for density-driven convection in underlying aquifers and are important landscape components because of their proximity to populated areas and/or important water resources. Examples of engineered water management systems with potential for density-driven convection include (1) recirculating cooling systems with ponds or canals for thermoelectric power plants, (2) industrial waste disposal facilities, and (3) land-based saltwater aquaculture facilities. Recirculating cooling systems at thermoelectric power plants are of interest because they are common in populated areas, have high evaporation rates, and are the third largest consumptive water use after irrigation and industrial sectors (Yang and Dziegielewski 2007). There are 85 thermoelectric plants in the USA that utilize recirculating cooling ponds or canals (US Department of Energy 2005) with a total capacity of approximately 400,000 megawatt-hours of electricity (MWe-hr) and a maximum water consumption of 5,300 $L(MWe\text{-}hr)^{-1}$ (King et al 2008). In addition to increased salinities in thermoelectric cooling ponds and canals resulting from enhanced evaporation, these systems typically have temperatures that exceed ambient air temperatures by several degrees Celsius (°C) or more; these elevated temperatures decrease fluid density and can stabilize the effects of increased salinity.

Density-driven flow processes in saline systems and industrial waste disposal facilities have been evaluated conceptually and numerically by a number of researchers (e.g., Fan et al. 1997; Holzbecher 2005; Nield et al. 2008; Oostrom et al. 1992; Sanford and Wood 2001; Simmons et al. 1999). Thermohaline density-driven convection in porous media has also been evaluated by numerous researchers for

Received: 15 December 2008 / Accepted: 2 July 2009

J. D. Hughes (✉)
US Geological Survey,
Florida Integrated Science Center,
10500 University Center Drive, suite 215, Tampa, 33612 FL, USA
e-mail: jdhughes@usgs.gov

C. D. Langevin · L. Brakefield-Goswami
US Geological Survey,
Florida Integrated Science Center,
3110 SW 9th Avenue, Ft. Lauderdale, 33315 FL, USA

Published online: 12 August 2009

DOI 10.1007/s10040-009-0502-7

idealized systems with simple boundary conditions and conceptual permeability configurations (Chen and Chen 1993; Diersch and Kolditz 1998; Griffiths 1981; Nield 1968; Oldenburg and Pruess 1998; Rubin 1982; Rubin and Roth 1979, 1983).

The combined effect of salinity and temperature differences and aquifer heterogeneity on density-driven convection was evaluated in the present study at a thermoelectric power plant in south Florida, USA. The power plant contains a large cooling canal system with warm hypersaline water overlying a highly permeable limestone aquifer. The salinity of the cooling water is significantly greater than natural groundwater salinities in the area, and thus, the presence of unstable density-driven convection is likely. The potential for unstable density-driven convection is somewhat diminished, however, by cooling water temperatures that are significantly greater than local groundwater temperatures. The site is important because the facility is located in the vicinity of several public water supply well fields, adjacent to sensitive ecological areas, and near the freshwater/saltwater interface.

Representative geometric and hydrologic characteristics of the site and surrounding area were used to develop a simplified two-dimensional cross-sectional model of variable-density groundwater flow, solute transport, and heat transport. As this work presents a first assessment on the hydrologic impacts of these types of cooling systems, the model was not calibrated, but was instead used to examine sensitive hydrogeologic parameters, to provide insight into the hydrologic effect of the cooling canals, and to provide guidance for monitoring and data collection at this site as well as other sites with similar density contrasts and hydraulic properties. Specifically, numerical results are used in this paper to determine (1) the behavior of density-driven convection, (2) the time required for high-salinity and high-temperature plumes to reach the bottom of the aquifer, (3) the aquifer salinization rate, and (4) the movement of the freshwater/saltwater interface. These factors were evaluated for different, but realistic, hydraulic conductivity configurations, initial salinity and temperature distributions, dependence of fluid density on temperature, cooling system salinity, and cooling system configurations.

General description of the study area

The study area is located at Turkey Point in southeastern Florida, USA (Fig. 1). Biscayne National Park, which includes much of the shallow Biscayne Bay marine estuary, lies east and northeast of the study area. Card Sound is east and southeast of Turkey Point, developed areas of Miami-Dade County are located to the northwest, and the Florida Everglades are directly west of the site. The study area has a subtropical climate with mean air temperatures ranging from 24.0 to 25.0°C, mean Biscayne Bay water temperatures ranging from 25.4 to 27.9°C, annual rainfall ranging from 1,270 to 1,524 mm, and annual evapotranspiration ranging from 1,077 to 1,301 mm (German 2000).

The Turkey Point power generation facility is operated by Florida Power and Light and supplies electricity to south Florida. The facility includes two nuclear and two fossil fuel generation units with a 2,324 MWe-hr capacity rating (US Department of Energy 2000). A closed-loop cooling canal system (CCS) covering 28 km^2 is used to cool non-contact cooling water from the nuclear and fossil fuel generation units (Gaby et al. 1985).

Specifics of the CCS are detailed in US Nuclear Regulation Commission (2002) and are summarized below. At its maximum extent, the CCS consists of 32 canals that carry warm water south from the plant and 8 canals that return water to the plant (Fig. 1). The canals, separated by 27-m-wide berms, are approximately 60 m wide with water depths ranging from 0.3 to 1 m. The easternmost canal was excavated to approximately 5.5 m below mean sea level (H. A. Frediani, Jr., Golder Associates, Inc., personal communication, 2008). The berms were created from material dredged during canal construction, and range from 1 to 5 m in height (Gaby et al. 1985). Maximum water temperatures range from 28 to 43°C where plant discharge occurs and are reduced approximately 2°C, ranging between 27 to 41°C, after traveling the nearly 270 km length of the CCS back to the plant intake (US Department of Energy 2000).

The canal system does not discharge directly to fresh or marine surface waters. Makeup cooling water for the canal system, required to replace evaporative losses, comes from treated process water, incident rainfall, stormwater runoff, and likely groundwater inflows (Florida Power and Light 2000). Exchange of water between the canal system and groundwater is likely because the canals are unlined. An interceptor canal is located along the west side of the canal system (Fig. 1) and is used to create an artificial groundwater gradient from the area west of the CCS into the ditch by pumping water from the interceptor canal into the CCS during the dry season. This is intended to prevent shallow westward flow of hypersaline water from the cooling canals.

The study area is underlain by an unconfined surficial aquifer system that includes a layer of peat, muck, marl, and/or fill and the underlying Pliocene-Pleistocene Biscayne aquifer composed of porous limestone (Cunningham et al. 2006). The vertical extent of the Biscayne aquifer is defined as areas where highly permeable materials are at least 3 m thick and have a minimum hydraulic conductivity of 300 m/day (Fish 1988). The upper peat, muck, marl, and/or fill materials are generally less than 2 m thick (Reese and Cunningham 2000) and have hydraulic conductivities ranging from 0.12 to 12 m/day for 12 distinct soil types in the study area (Noble et al. 1996). The bulk hydraulic conductivity of the Biscayne aquifer in the vicinity of the study area ranges from approximately 2,700 to 7,300 m/day (Fish and Stewart 1991). Cunningham et al. (2006) measured hydraulic conductivities ranging from 0.001 to 22,929 m/day and determined lithofacies-based median horizontal hydraulic conductivities for low permeability (480 m/day), moderate permeability (2,300 m/day), and high permeability (7,000 m/day) portions of the Biscayne

DOI 10.1007/s10040-009-0502-7

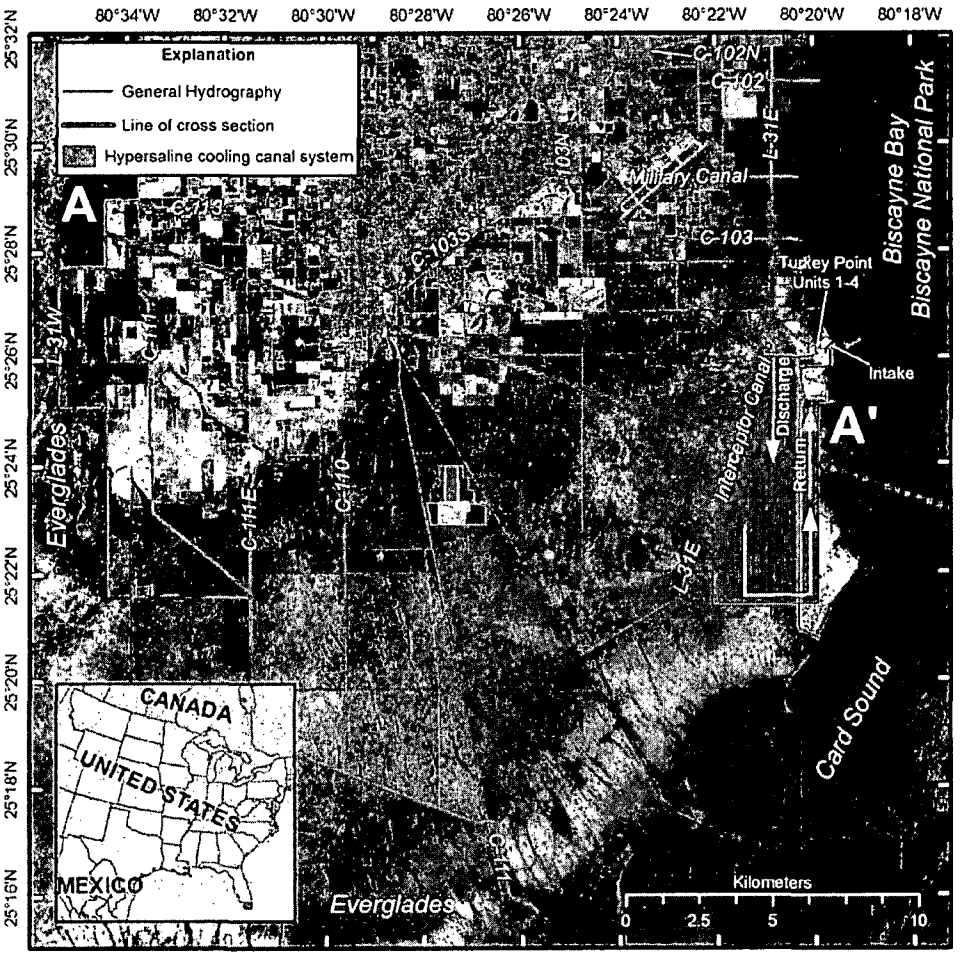

Fig. 1 Location of study area and two-dimensional cross-section model developed for the Turkey Point hypersaline cooling canal system. The line of cross section (*red*) does not show the full extent of the model and has been *dashed* in offshore areas of the model. The cross-section model extends approximately 15,500 m further offshore. General hypersaline cooling canal system flow directions (*orange*, *yellow* and *green arrows*) and the location of the discharge canals, return canals, intake canal, and power generation units are shown

aquifer; the Cunningham et al. (2006) work was conducted in western portions of the study area and has been applied in numerical models developed for the area (Shoemaker et al. 2008). High permeability values are characteristic within thin (decimeter-scale), sheet-like preferential flow layers of the Biscayne aquifer with touching vug porosity.

Simulation of the groundwater flow system

The SEAWAT model

The US Geological Survey computer program, SEAWAT (Guo and Langevin 2002; Langevin et al. 2003; Langevin and Guo 2006; Langevin et al. 2007), was used to simulate coupled heat transport, total dissolved solids (TDS) transport, and groundwater flow in the Biscayne aquifer. The latest SEAWAT version (Version 4; Langevin et al. 2007) couples MODFLOW-2000 (Harbaugh et al. 2000) with MT3DMS (Zheng and Wang 1999) and allows density to be calculated as a function of one or more solute species and temperature. Use of SEAWAT to simulate heat transport is limited to evaluation of fully saturated porous media. Dausman et al. (2009) tested this latest version by simulating six solute and heat transport benchmark problems. Langevin et al. (2009) performed additional testing by simulating a laboratory experiment in which warm freshwater was used to recharge a large sand-filled glass tank with a cold saltwater reservoir at one end.

Model construction

The model developed for this study is patterned after the geometric configuration and hydrologic conditions of the CCS at Turkey Point. In many instances, details on the specific hydrologic conditions at the site were unavailable, including a description of aquifer hydraulic properties. For this reason, the numerical analysis presented here focuses on identifying the important physical processes and controls on density-driven convection and aquifer salinization for a variety of realistic hydraulic conductivity configurations.

DOI 10.1007/s10040-009-0502-7

The location of the cross-section model of the Biscayne aquifer for the study area is shown in Fig. 1. Aquifer and fluid properties used for the simulations are summarized in Table 1. The cross-section model is approximately 46 km in length and is discretized using a total of 718 columns horizontally and 30 layers vertically (21,540 active grid cells) using the model grid shown in Fig. 2. Column widths vary from 10 m in the area of the CCS and increase to 200 m in western portions of the model, in Biscayne Bay, and further offshore in the Atlantic Ocean. A constant layer thickness of 1 m was used throughout the model domain.

A number of different hydraulic conductivity configurations were evaluated and are discussed in detail in the following section. An effective porosity of 0.20 was used in all grid cells and is comparable to the median total porosity (0.24) measured by Cunningham et al. (2006) in 267 Biscayne aquifer core samples. Specific yield and specific storage values were set to zero in the cross-section model for all simulations. This simplifying assumption was used because the primary objective of the cross-section model is to evaluate the relative response of the system to a number of plausible hydraulic conductivity and boundary condition configurations. The interceptor canal was constructed to reduce the effect of the CCS on groundwater levels. As a result, it is expected that average water levels in the Biscayne aquifer have not changed noticeably and storage changes have been minimal. Changes in groundwater in storage would result in longer aquifer response times than simulated in the present model but relative differences in transport times between different hydraulic conductivity configurations would remain the same. As a result, simulated results represent a conservative estimate of transport times.

Boundary conditions, the types and locations of which can be seen in Fig. 2, were assigned in the cross-section model based on average conditions in the study area. A freshwater constant head, constant temperature boundary was specified in model layers 1 through 30 on the western boundary (column 1) of the model based on average Biscayne aquifer water levels and temperature (Langevin 2001). Aquifer recharge and discharge, which exhibit a strong seasonal component, were not represented for the agricultural areas and coastal wetlands located between the western model boundary and L-31E. Instead, a no-flux condition (for flow and transport) was specified for the model surface and groundwater flow was represented as confined flow. This simplification results in regional groundwater flow entering solely from the western boundary and does not consider small spatial and temporal variations in local recharge. Head-dependent flux boundary conditions (GHB) with constant temperatures were specified for canal L-31E and the interceptor canal in model layer 1 based on Dames and Moore (1989) and Langevin (2001, 2003). GHBs with constant TDS concentrations and temperatures were specified in model layer 1 for the CCS (US Department of Energy 2000); CCS GHBs for the eastern canal were extended to model

Table 1 Model parameters used in the two-dimensional cross-section model

Freshwater TDS concentration	$C_0 = C_{fw} = 0.000$[‰]
Seawater TDS concentration	$C_{sw} = 35$[‰]
Cooling canal TDS concentration	$C_{cp} = 70$[‰] (base case)
Freshwater fluid density	$\rho_{fw} = 998.2\,[kg/m^3]$ at 20°C
Saltwater fluid density	$\rho_{sw} = 1,024.5\,[kg/m^3]$ at 20°C
Cooling canal fluid density	$\rho_{cp} = 1,050.7\,[kg/m^3]$ at 20°C(base case)
Fluid density-TDS concentration relation	$\frac{\partial \rho}{\partial C} = 0.75$ [kg / (°/oo m^3)]
Reference temperature	$T_0 = 20$[°C]
Land surface temperature	$T_{Land} = 24.4$[°C]
Seawater temperature	$T_{Seawater} = 26.2$[°C]
Cooling canal fluid temperature	$T_{cp} = 35.6$ [°C] (discharge) or 34.2 [°C] (return)
Fluid density-temperature relation	$\frac{\partial \rho}{\partial T} = -0.375\,[kg/(°Cm^3)]$ (base case)
Reference viscosity	$\mu_0 = 0.001[kg/(ms)]$
Viscosity-temperature relation	$\frac{\partial \mu}{\partial T} = .0[kg/(ms)]$
Longitudinal dispersivity	$\alpha_L = 5$ [m]
Horizontal transverse dispersivity	$\alpha_T = 0.5$ [m]
Vertical transverse dispersivity	$\alpha_V = 0.5$ [m]
Molecular diffusion coefficient for salt	$D_M = 1.477 \times 10^{-9}\,[m^2/s]$
Distribution coefficient for salt	$K_{DC} = 0.0000\,[m^3/kg]$
Porosity	$\theta = 0.2$ [-]
Solid matrix density	$\rho_{SOLID} = 2,710\,[kg/m^3]$
Specific heat of the fluid	$c_F = 4,183.[J/(kg°C)]$
Specific heat of the solid	$c_S = 835[J/(kg°C)]$
Distribution coefficient for temperature	$K_{DT} = 2.0000 \times 10^{-4}\,[m^3/kg]$
Thermal conductivity of fluid	$\lambda_W = 0.61[J/(m°Cs)]$
Thermal conductivity of solid	$\lambda_S = 3.59[J/(m°Cs)]$
Bulk thermal conductivity	$\lambda_{Bulk} = 2.994[J/(m°Cs)]$
Bulk thermal diffusivity	$D_T = 3.5788 \times 10^{-6}\,[m^2/s]$

DOI 10.1007/s10040-009-0502-7

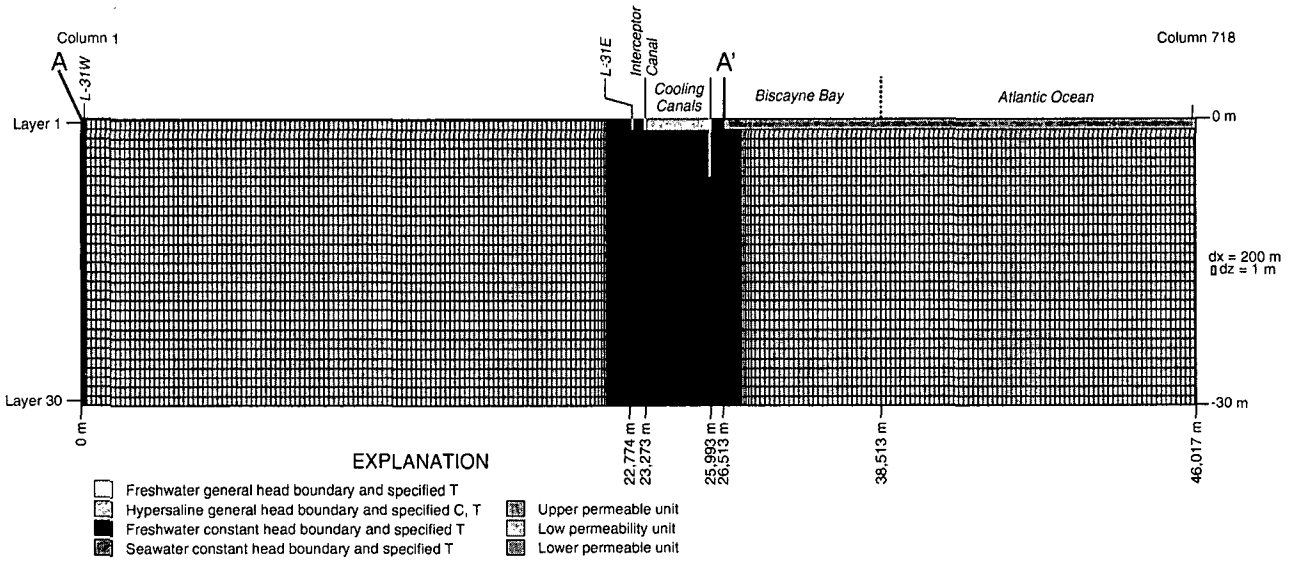

Fig. 2 Model grid, boundary conditions, and hydraulic conductivity zones evaluated. The location *A* to *A'* in the two-dimensional cross-section model is shown in Table 1. Model parameters used in the two-dimensional cross-section model and the hydraulic conductivity values associated with each hydraulic unit is summarized in Table 2

layer 6 to represent its deeper connection with the Biscayne aquifer (H. A. Frediani, Jr., Golder Associates, Inc., personal communication, 2008). Constant TDS concentrations were specified for the CCS GHBs based on an assumption that these features would always be a source of salt as a result of (1) enhanced evaporation from the system because of the thermal contrast between CCS water and the atmosphere (2) use of makeup water sourced from seepage of saltwater from Biscayne Bay, and (3) recirculation of CCS water captured by the interceptor canal and pumped back into the cooling canals. An upper TDS concentration of 70‰ was assigned for the CCS based on unpublished Florida Power and Light quarterly reports containing measured groundwater salinities in monitoring wells adjacent to the site. A lower TDS concentration of 35‰ was also tested.

For the range of TDS concentrations and temperatures evaluated, density variations resulting from maximum temperature variations are not sufficient to compensate for density variations resulting from TDS concentrations. Density variations resulting from the maximum range of TDS concentrations of 70 and 35‰ are 52.5 and 26.3 kg/m^3, respectively. Conversely, density variations resulting from the maximum range of temperatures (land surface temperature – discharge CCS fluid temperature = 11.2 °C) is −4.2 kg/m^3.

Exchange between GHBs and the Biscayne aquifer is controlled by a conductance value and the simulated difference between the specified GHB head and simulated head in the grid cell. GHB conductance values were calculated as the product of the exchange area ($\Delta x \cdot \Delta y$), a hydraulic conductivity of 3 m/day, and a simulated connection distance between the grid cell and GHB of 1 m. The values for Δx and Δy underneath the CCS are 10 and 30 m, respectively. A constant head, constant temperature seawater boundary was specified along the eastern portion of the model (columns 568–718) in model layer 1 based on Langevin (2001). Since the Biscayne aquifer is an unconfined aquifer and the model was extended 20 km offshore, a zero-flux boundary was defined for model layers 2–30 on the eastern side of the model. All other boundaries are defined as no flux boundaries. Heads, TDS concentrations, and temperatures specified for boundary conditions are shown graphically in Fig. 3.

An upstream weighted, finite-difference numerical transport scheme was used to simulate TDS and heat transport. The model was run for a total of 18,250 days (50 years) with three periods (MODFLOW stress periods) having lengths of 9,125 days, 1 day, and 9,124 days in order to represent unique boundary condition configurations and/or specific maximum time-step lengths. Maximum time step lengths of 1 day, 0.1 days, and 1 day were used for MODFLOW stress period 1, 2 and 3, respectively. Flow and transport were explicitly coupled for the simulations using a one time-step lag. GHBs and associated constant TDS concentration and temperature boundary conditions representing the CCS were not active during the first MODFLOW stress period in order to achieve steady-state conditions consistent with defined lateral boundary conditions and aquifer properties used in the simulation. Heads, TDS concentrations, and temperatures from previous simulations run to steady-state without the CCS were used to define initial conditions for all of the simulations.

The total length of MODFLOW stress periods 2 and 3 (25 years) is roughly based on completion of the CCS in 1974 (Gaby et al. 1985) and use of cooling canal data for the year 2000 (US Department of Energy 2000) rather than running the simulations to steady-state. The length of MODFLOW stress period 2 was restricted to a single day to better resolve the initial progression of seepage from the base of the CCS.

DOI 10.1007/s10040-009-0502-7

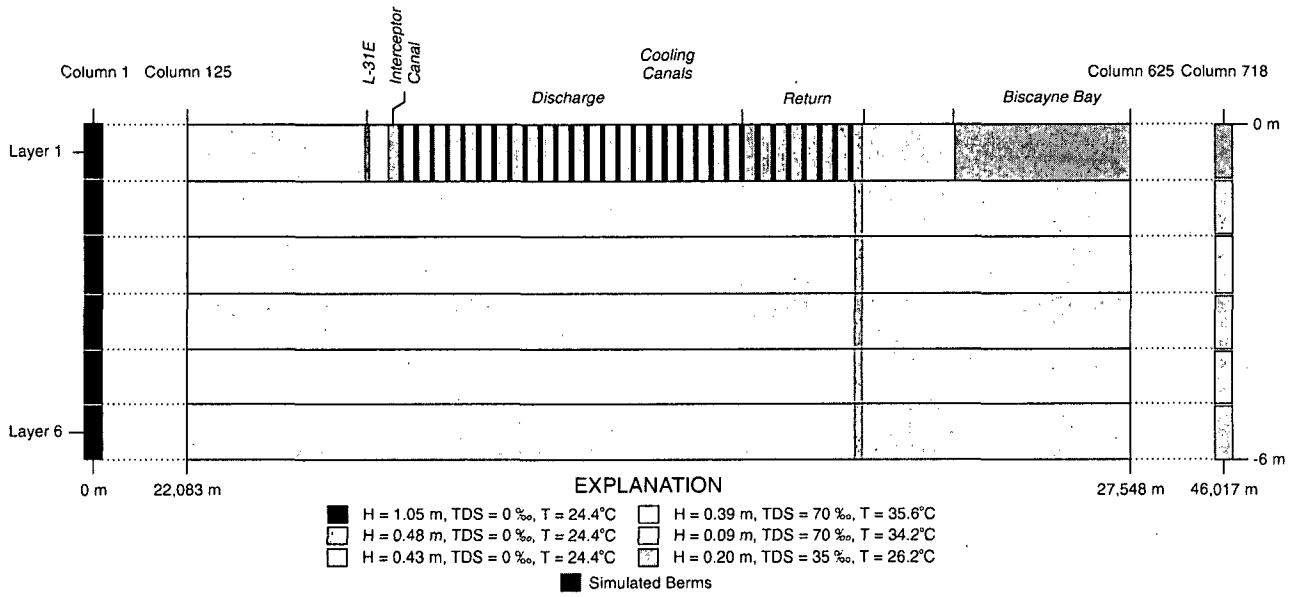

Fig. 3 Configuration of boundary condition heads, TDS concentrations, and temperatures in the vicinity of the cooling canal system in the two-dimensional cross-sectional model

Model results

The two-dimensional cross-section model was used to evaluate the effects of hydraulic heterogeneities, cooling canal TDS concentrations, heat transport, and cooling canal geometry on seepage of saline to hypersaline water from the CCS and movement of the freshwater/saltwater interface. The cumulative effects of hydraulic conductivity heterogeneities in combination with cooling canal TDS concentrations, heat transport, or cooling canal geometry were considered and are discussed in detail below. The effect of TDS concentration and temperature on fluid viscosity was not evaluated; the reference fluid viscosity shown in Table 1 was used in all simulations. Because hydraulic conductivity is a function of the ratio of fluid density (ρ) to fluid viscosity (μ) and the reference fluid viscosity (μ_o) was used in all simulations, simulated results represent a conservative estimate of groundwater flow induced by elevated TDS concentrations and temperatures in the CCS. Simulations evaluating the effects of hydraulic conductivity, where fluid density is a function of TDS concentrations and temperature, are referred to as "base simulations." These "base simulations" are referred to in subsequent analyses of the effects of cooling canal TDS concentrations, heat transport, and cooling canal geometry on seepage of hypersaline water from the CCS and the position of the freshwater/saltwater interface.

Effects of aquifer heterogeneity on cooling canal seepage

Four different hydraulic conductivity configurations were evaluated to determine the effects on cooling canal seepage and the position of the freshwater/saltwater interface. Fluid density in these simulations is a function of TDS concentrations and temperature using the parameters defined in Table 1. Hydraulic conductivity in the model was discretized into upper and lower permeable units with intervening units that can serve as low permeability confining units (Fig. 2). Hydraulic conductivity values used in the defined permeability units in cases A, B, C, and D, as summarized in Table 2, are within the range of values reported by Cunningham et al. (2006), Fish (1988), and Noble et al. (1996). The configuration evaluated in case C and D is comparable to the hydrogeologic framework in western portions of the study area (Cunningham et al. 2006).

The spacing of canals and berms in the CCS establishes a horizontally perturbed, unstable density configuration that in combination with high aquifer

Table 2 Hydraulic conductivity configurations evaluated with the two-dimensional cross-section model

Hydraulic unit	Case A	Case B	Case C	Case D
Upper permeable unit	K_h=10,000	K_h=1,000	K_h=1,000	K_h=1
	K_v=100	K_v=10	K_v=10	K_v=0.1
Low permeability unit	K_h=10,000	K_h=1,000	K_h=1	K_h=1
	K_v=100	K_v=10	K_v=1	K_v=1
Lower permeable unit	K_h=10,000	K_h=1,000	K_h=1,000	K_h=1,000
	K_v=100	K_v=10	K_v=10	K_v=10

Horizontal and vertical hydraulic conductivity (m/day) are shown for each case. The spatial distribution of defined hydraulic units is shown in Fig. 2

DOI 10.1007/s10040-009-0502-7

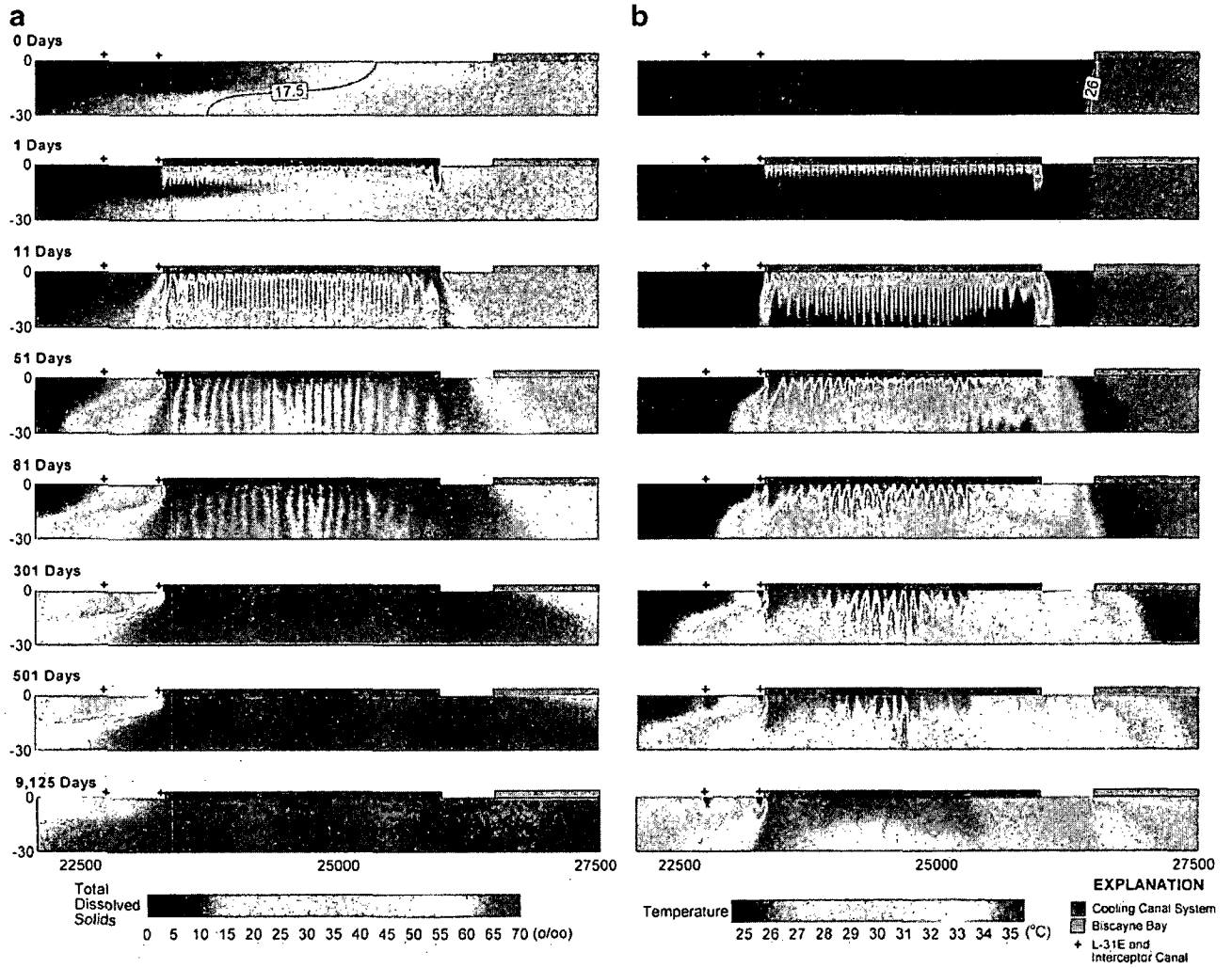

Fig. 4 **a** Simulated TDS concentrations (‰) and **b** temperatures for base simulation case A after specified days since cooling canal system construction

permeability, leads to the development of lobate-shaped hypersaline plumes (fingers). These finger plumes develop for all four hydraulic conductivity cases. For illustrative purposes, simulated TDS concentrations and temperatures for selected times in the immediate vicinity of the CCS are shown for case A (Fig. 4). Results prior to installation of the CCS show that fresh groundwater is discharging to L31-E and brackish groundwater is discharging to Biscayne Bay, the freshwater/saltwater interface is located in the vicinity of the CCS, and a convective saltwater flow system is developed seaward of the freshwater/saltwater interface. Hypersaline water begins to enter the Biscayne aquifer immediately after the CCS is installed and arrives at the base of the aquifer within 10 days. Unstable convective flow patterns result from the plumes descending downward into the aquifer; as the denser plumes descend relatively fresh groundwater is forced upward in the areas between the plumes. After about 300 days, all hypersaline plumes have reached the bottom of the aquifer and movement of hypersaline water is predominantly horizontal away from the CCS. Hypersaline water moves the position of the freshwater/saltwater interface landward, out of the extent of results shown in Fig. 4. The freshwater/saltwater interface does not reach steady-state east of the CCS at the end of the simulation.

Thermal finger plumes also develop for the four hydraulic conductivity cases. In general, these thermal plumes are more diffuse and move slower than the hypersaline plumes. As shown for case A, thermal plumes develop immediately after CCS installation and begin to arrive at the base of the aquifer within about 10 days (Fig. 4). Distinct thermal finger plumes persist for at least 500 days. Vertical heat transport is not as rapid as vertical salt transport in the simulation with temperatures less than specified CCS temperatures at the base of the aquifer observed at the end of the simulation. The lateral extent of the aquifer affected by the thermal plume is less than the extent affected by the hypersaline plume as a result of specified temperature boundaries for L-31E, the interceptor canal, and Biscayne Bay.

Simulation results for cases B, C, and D also show development of hypersaline finger plumes, the primary

DOI 10.1007/s10040-009-0502-7

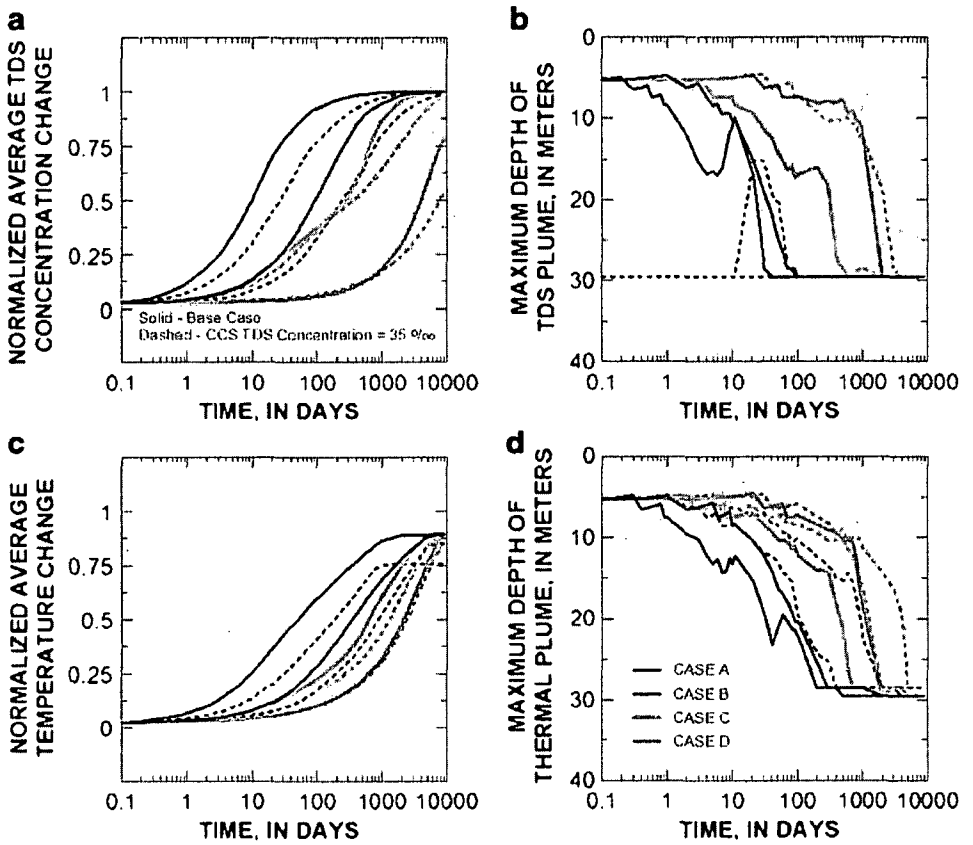

Fig. 5 Simulated **a** normalized average TDS concentration, **b** maximum depth of TDS plume concentration, **c** temperature changes and **d** maximum depth of thermal plumes directly below the CCS

difference between the four cases being the rates of vertical mass transfer and aquifer salinization. The normalized average TDS concentration change $[(C - C_{t=0})/(C_{cp} - C_{t=0})]$ was calculated for the aquifer domain directly beneath the CCS and is plotted in Fig. 5a as a function of time. All cases yield a similar temporal pattern in the increase of average TDS concentration. The aquifer becomes entirely hypersaline beneath the CCS for cases A, B, and C. For case D (the lowest permeability case), the aquifer does not become entirely hypersaline within the simulation period, but it appears that it would do so if given enough time. Maximum hypersaline plume depth beneath the CCS is shown in Fig. 5b as a function of time. For cases A and B, hypersaline plumes reach the bottom of the aquifer in less than 100 days; for cases B and C, the plumes arrive at the base of the aquifer after about 600 and 2000 days, respectively. The apparent upward movement of the TDS plume for case A (Fig. 5b) is caused by the easternmost plume moving outside of the analysis window, which is confined to the area directly beneath the CCS. These results quantify the importance of hydraulic conductivity on rates of aquifer salinization beneath the CCS.

The normalized average aquifer temperature change $[(T - T_{t=0})/(T_{cp} - T_{t=0})]$ beneath the CCS is shown for all four cases in Fig. 5c. Heating of the aquifer to the specified CCS temperature is clearly delayed compared to the aquifer salinization process (compare Fig. 5c with a). This delay occurs due to the thermal equilibration between the solid aquifer matrix and the ambient groundwater. As the thermal plumes sink downward through the aquifer, vertical movement is delayed by the transfer of thermal energy from the water to the aquifer matrix. The delay is not observed for the hypersaline finger plumes because salt is not absorbed by the aquifer matrix. Comparison of the maximum thermal plume depth (Fig. 5d) with the maximum hypersaline plume depth (Fig. 5b) also shows that the thermal plumes tend to move slower than the hypersaline plumes.

Average simulated GHB flow rates for cases A, B, C, and D are 58, 10, 7.9, and 0.38 mm/day, respectively. GHB flow rates exceed the difference between average daily rainfall (3.5–4.2 mm/day) and evapotranspiration (2.9 to 3.6 mm/day) rates for cases A, B, and C and indicate inflows to the CCS from plant discharge and groundwater seepage from Biscayne Bay would have to be on the order of GHB flow rates or higher to maintain CCS water levels. At a maximum plant discharge of 580 mm/day (Lyerly 1998), maximum GHB flow rates (case A) would represent approximately 10% of the plant discharge to the CCS.

Increase in aquifer salt content and position of the freshwater/saltwater interface

The effect of the CCS on the increase in total aquifer salt content is shown in Fig. 6. Use of the total aquifer salt

DOI 10.1007/s10040-009-0502-7

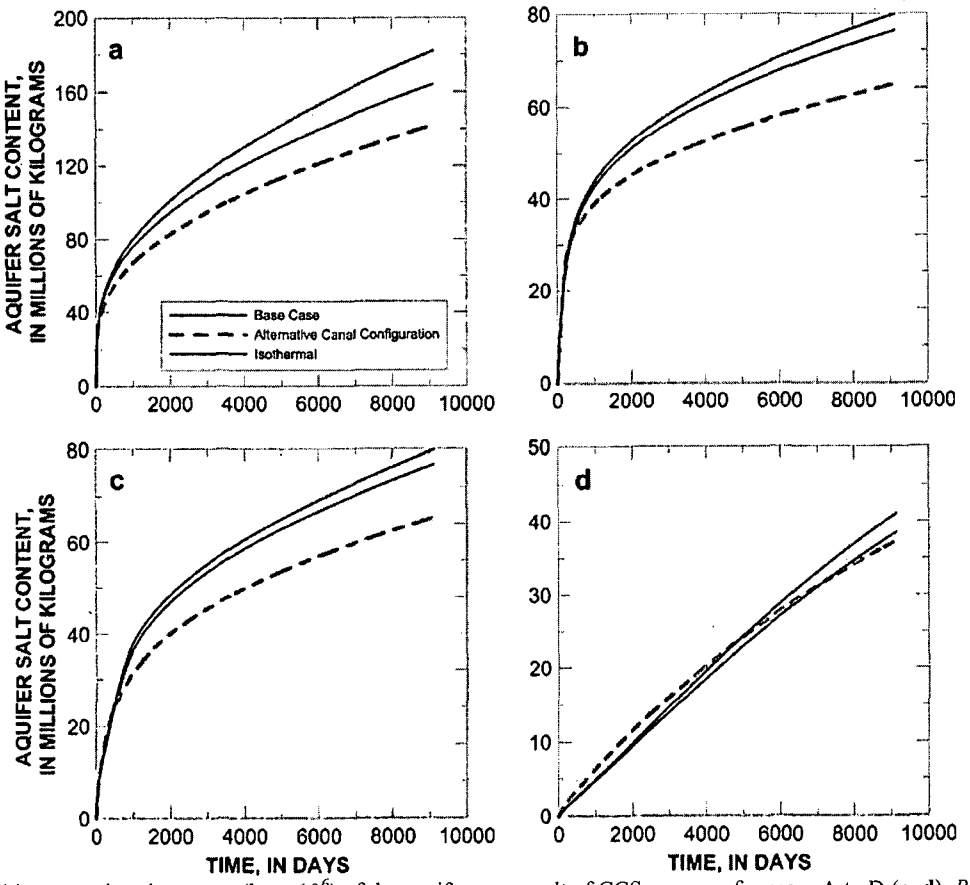

Fig. 6 Simulated increases in salt content (kg × 10^6) of the aquifer as a result of CCS seepage, for cases A to D (**a–d**). *Base case* refers to simulations with canal TDS concentrations of 70‰. The *alternative canal configuration* simulation setup is the same as the base case except berms separating canals have been removed. The *isothermal* simulation setup is the same as the base case except temperature does not affect fluid density

content here is intended to evaluate aquifer salinization over the entire length of the cross section; in the previous section, the aquifer salinization focused on the area directly beneath the CCS. Increases in total salt content provide another measure of hypersaline water seepage from the CCS to the aquifer. Salt content results indicate that the salt increase for case A is approximately a factor of 2 greater than case B and C and approximately a factor of 4 greater than case D. In cases A, B, and C, approximately one half of the salt increase occurs in the first 1,000 days and asymptotically increases over the remainder of the simulation period. The increase in the salt content of the aquifer is roughly linear over the entire simulation period for case D.

The effect of the CCS on the position of the 1‰ TDS concentration at the base of the aquifer is shown in Fig. 7. Horizontal distances of this contour are measured relative to the starting location at the base of the aquifer prior to CCS installation. The relative movement of the 1‰ TDS concentration is greatest (12,000 m) for case A with this case yielding movement approximately 4 times greater than case B and C and a factor of 30 greater than case D. Movement of 1‰ TDS concentration also occurs quickly in case A. Movement of the position of the 1‰ TDS concentration is limited until approximately 1,000 and 2,000 days in cases B and C, respectively, and is roughly linear. Movement of the 1‰ TDS concentration in case D is slow until approximately 5,000 days and is roughly linear until the end of the simulation.

Effects of TDS concentrations on cooling canal seepage

To evaluate the effect of CCS salinity on aquifer salinization, the four hydraulic conductivity configurations were also simulated using a CCS salinity value equal to seawater (35‰) instead of the hypersaline value (70‰) used in the base simulations. Compared to the base simulations, these simulations with a seawater salinity CCS also show lobate-shaped salt fingers descending downward into the aquifer; however, the fingers descend slower because of the reduced density contrast between the CCS and ambient groundwater. Aquifer salinization is also slower for these cases simply because the TDS concentration of the CCS was halved. These points are evident in Fig. 5a. For cases A, B, and C, normalized average TDS concentration changes beneath the CCS reach 70‰ between 100 and 1,000 days. In contrast, the normalized average TDS concentration change does not approach 35‰ for these cases until after 1,000 days.

DOI 10.1007/s10040-009-0502-7

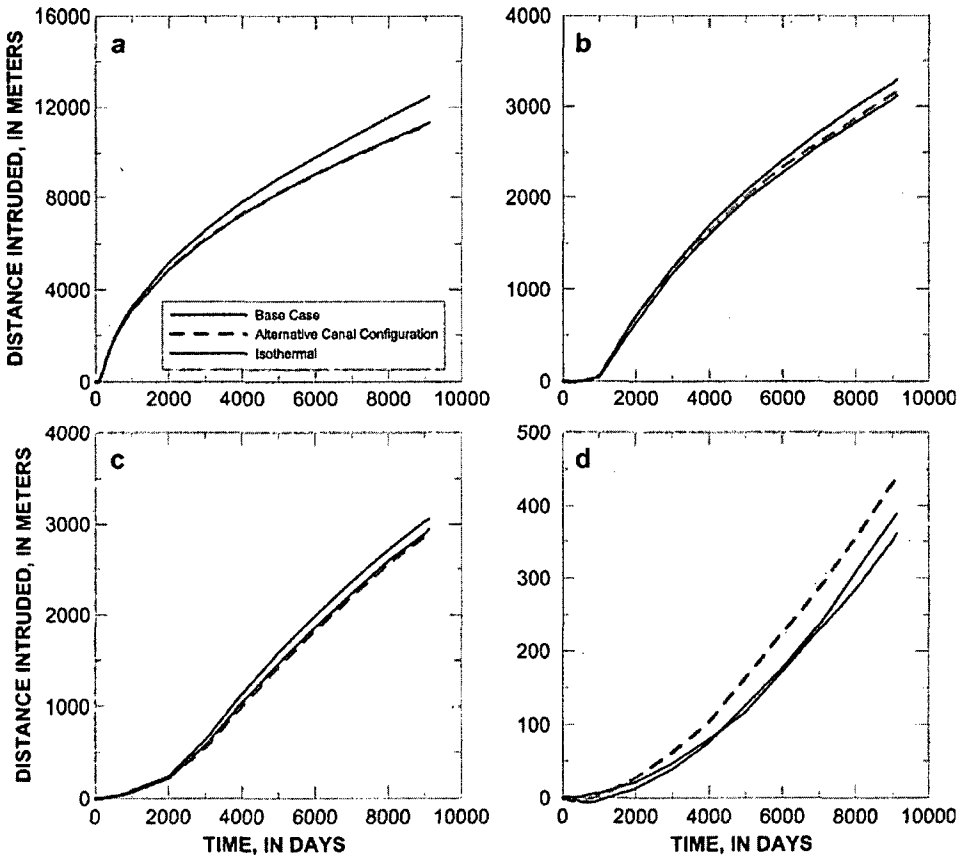

Fig. 7 Simulated movement of the 1‰ TDS concentration at the base of the aquifer. Results for the CCS with and without the dependence of fluid density on temperature and the Alternative CCS (cooling canal system) with the dependence of fluid density on temperature are shown for cases A to D (**a–d**)

Plots of aquifer salt content and movement of the 1‰ TDS concentration at the base of the aquifer are shown in Fig. 8. Although downward plume movement is generally slower for the seawater salinity CCS simulations (Fig. 5b, d), the aquifer salt content reaches equilibrium faster than for the equivalent base simulations. Initial values for the maximum depth of the TDS plume (Fig. 5b) for cases A and B with a CCS TDS concentration of 35‰ are a result of the presence of saltwater at the base of the aquifer when the CCS is installed. Fig. 8a shows that the aquifer salt content for case A reached equilibrium within about 10 years, and that the content for cases B, C, and D is approaching equilibrium by the end of the simulation. In contrast, none of the base simulations reached equilibrium in aquifer salt content within the 25-year simulation (Fig. 6). Total salt accumulation within the aquifer for the 35‰ CCS simulations is much less than the salt accumulation for the base simulations. Differences in aquifer salt content between the 35 and 70‰ base simulations by a factor of 2 would be expected and explained simply by the concentration difference of the CCS seepage. However, the salt content at the end of the simulation for the case A base simulation (160×10^6 kg) is more than 10 times larger than the salt content with a 35‰ CCS (15×10^6 kg). This means that the average CCS seepage rate for the hypersaline base simulation is about 5 times greater than the average seepage rate for seawater salinity cooling canals. The other hydraulic conductivity cases show similar relations. Salt accumulation for the base simulations are between 6 and 8 times greater than the same cases with seawater salinity canals.

Simulation results indicate that inland movement of the saltwater interface at the base of the aquifer is highly sensitive to the TDS concentration of the CCS. For example, in the case A simulation with seawater salinity cooling canals, the interface reached an equilibrium position almost 2 km inland from its initial position after about 10 years (Fig. 8b). This is less than the 2-km width of the CCS because water levels on the western side of the canals are higher than sea level by 0.19 m. For the same case with a hypersaline CCS, the saltwater interface moved inland by almost 12 km after 25 years, but had not yet reached its equilibrium position. Thus, for this particular hydraulic conductivity case, doubling the TDS concentration of the CCS resulted in the interface moving farther inland by at least a factor of 6.

For the lowest hydraulic conductivity case (case D), there is a pronounced movement of the toe in the opposite (seaward) direction, at least for the 25-year simulation period (Fig. 8b). Most of the other cases also show this curious response, but the response is so slight that it cannot be seen in the plots. Although this response is

DOI 10.1007/s10040-009-0502-7

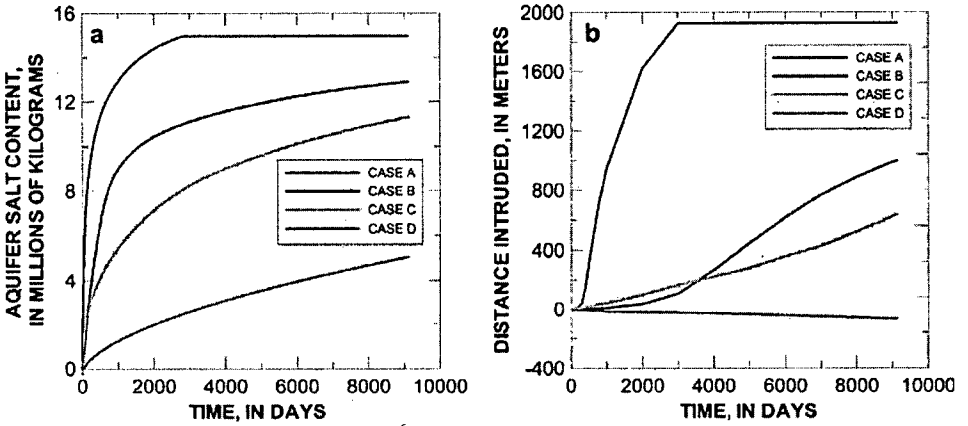

Fig. 8 Simulated **a** increases in aquifer salt content ($kg \times 10^6$) and **b** movement of the 1‰ TDS concentration at the base of the aquifer for simulations with specified cooling canal TDS concentrations of 35‰

counterintuitive, it can be explained as a transient response to the redirection of freshwater outflow. As the saline fingers descend from the base of the CCS, the natural outflow face to Biscayne Bay becomes hydraulically separated from the regional flow system. As this occurs, regional freshwater flow is redirected into surface water features inland of the CCS. This redirection causes the saltwater interface to be temporarily eroded by freshwater. With the exception of case D with seawater salinity cooling canals, movement of the freshwater/saltwater interface eventually proceeds as saline water from the CCS reaches the bottom of the aquifer and moves inland.

Effects of heat on cooling canal seepage

The importance of temperature variations on canal seepage and groundwater flow patterns was evaluated by eliminating the dependence of fluid density on temperature and comparing results with the base simulations. Although heat transport was represented in these simulations, they are referred to here as "isothermal" in Figs. 6 and 7 because simulated temperatures do not affect groundwater flow. This analysis does not consider the effect of cooling canal temperature on evaporation, which is thought to be an important component of the CCS water budget.

In general, temperature variations have only a minor affect on seepage rates, flow patterns, and the time for normalized average TDS concentration changes to achieve maximum concentrations beneath the CCS (Fig. 9). The increase in aquifer salt content over time, however, shows a measurable response to the effects of temperature (Fig. 6). For case A, aquifer salt content is about 10% less at the end of the simulation when the effects of temperature are included. For cases B, C, and D, the percentage is less (5, 4, and 6%, respectively). Saltwater intrusion also shows a measurable response to the effects of temperature (Fig. 7). When temperature effects are neglected, the interface moves farther inland by a distance of 1,141, 175, 113, and 28 m for cases A, B, C, and D, respectively.

Effects of cooling system geometry on cooling canal seepage

The existing configuration of canals and berms in the CCS establishes a horizontally perturbed, unstable density configuration that leads to the development of lobate-shaped hypersaline plumes and increases vertical mass-transfer rates. To evaluate the effect of the geometry of the CCS on seepage of hypersaline water into the aquifer, an alternative geometric configuration (alternative CCS) that eliminates the horizontal perturbed density configuration was simulated. For this alternative case, the cooling system was assumed to be composed of a contiguous pond, segregated into discharge and intake portions, and covering the combined area of canals and berms in the CCS. To ensure that TDS mass flux was comparable to the flux observed in the base simulations GHB conductance was scaled by the ratio of the canals in the CCS and the total area of canals and berms in the CCS. Specified GHB heads, TDS concentrations, and temperatures are identical to those used in the base simulations (see Fig. 3).

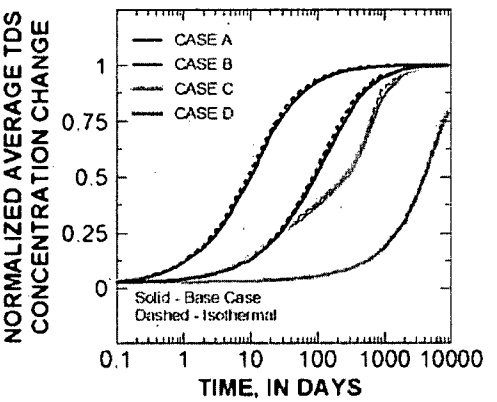

Fig. 9 Simulated normalized average TDS concentration changes directly below the CCS for the base and isothermal simulations

DOI 10.1007/s10040-009-0502-7

The temporal and vertical progression of hypersaline and relatively high temperature water in alternative CCS simulations for hydraulic conductivity configuration cases A, B, C, and D is comparable to the base simulations. Alternative CCS case D exhibited the greatest difference; seepage from alternative CCS was concentrated in the eastern end of the discharge portion of the CCS and increased the horizontal extent of the predominant area of vertical movement of hypersaline and high temperature water by approximately 500 m. Distinct hypersaline and thermal plumes were not as well developed in alternative CCS simulations. Differences in simulated times for hypersaline and thermal plumes to reach the bottom of the aquifer, mass transfer, and movement of the freshwater/saltwater interface is a result of larger perturbation wavelengths in the alternative CCS simulation which reduce instability development and vertical mass transfer (Menand and Woods 2005).

The effect of the alternative CCS on the salt content of the aquifer is shown in Fig. 6. Relative to the base simulations, initial salt increases (prior to 400 days) are slightly larger, as a result of the larger area of the CCS. Furthermore, the maximum aquifer salt increase is less for cases A, B, and C by approximately 12, 13, and 15%, respectively, as a result of decreased hypersaline and thermal plume development. The maximum aquifer salt increase is comparable in alternative CCS case D and the base case D simulation; initial aquifer salt content increases are slightly larger in alternative CCS case D until approximately 7,500 days as a result of the increased horizontal extent of the CCS in this simulation. The temporal response of salt content increases in the aquifer is comparable to the base simulations.

The effect of the alternative CCS on the position of the 1‰ TDS concentration at the base of the aquifer is shown in Fig. 7. The relative movement of the 1‰ TDS concentration is comparable to the base simulation for cases A, B, and C as a result of similarity between the location of the western most hypersaline plumes in the base and alternative CCS simulations. The timing and magnitude of the relative movement of the 1‰ TDS concentration for alternative CCS case D is greater than the base simulation by approximately 2,000 days and 70 m, respectively. The difference between case D for the alternative CCS and the base simulation is a result of the increased area of vertical movement and concentration of seepage in the eastern end of the discharge portion of the alternative CCS.

Conclusions

This paper presents a first assessment of the aquifer salinization processes that occur beneath an engineered, hypersaline cooling canal system (CCS). The analysis is based on numerical simulations of coupled variable-density groundwater flow, solute transport, and heat transport. A simplified two-dimensional cross-section model was developed using geometric characteristics and general features of the CCS at the Turkey Point power plant in south Florida, USA.

All simulated scenarios were shown to exhibit dense fingering instabilities with fingers developing in response to advective and dispersive components related to GHB fluxes and specified CCS TDS concentrations and temperatures, respectively. For all of the conditions tested, aquifer salinization initially occurs from the formation of dense, hypersaline fingers that descend downward from the base of the CCS to the bottom of the 30-m thick aquifer. Rates of finger convection are highly controlled by the vertical hydraulic properties of the aquifer and by the density contrast between CCS water and groundwater. Fingers reach the aquifer bottom within a few days for the highest hydraulic conductivity case and not for more than 5 years for the lowest hydraulic conductivity case. Aquifer salinization continues after the fingers reach the aquifer bottom as the saline plume spreads seaward beneath the adjacent estuary and landward. For most cases evaluated, aquifer salt content did not reach equilibrium within the 25-year simulation period nor did the position of the freshwater/saltwater interface at the base of the aquifer. In general, CCS salinity had a large affect on aquifer salinization. Larger TDS concentrations naturally result in larger aquifer salinization rates because of the concentration values themselves; but they also result in increased salinization rates and extent of salinization because of the larger density contrast.

The formation of saline finger plumes is enhanced by the alternating canal and berm configuration of the CCS. When this geometry is explicitly included in the simulation, as it was for the base case simulations, fingers develop beneath each cooling canal. Simmons et al. (2001) noted a similar control on fingering in a simulation with alternating vertical zones of low and high hydraulic conductivity. That simulation showed a finger forming within each high conductivity zone.

Results of the simulations indicate that temperature has a mitigating effect on aquifer salinization by reducing the density contrast between the CCS and the aquifer. Isothermal simulations show a 4–10% increase in total aquifer salt content at the end of the 25-year simulation period when compared to equivalent simulations with temperature effects included. The extent of saltwater intrusion is also greater for isothermal simulations. Simulation results also indicate that thermal plumes are generally constrained to the horizontal extent of the CCS, suggesting that thermal conduction within the aquifer is an effective mechanism for dissipating thermal plumes. These results suggest that cooling system evaluations may require full solute and thermal evaluations for accurate impact assessment.

The large variation in aquifer salinization rates and extent for the different hydraulic conductivity configurations indicate that additional data is required before a formal assessment can be made on the effects of the CCS at Turkey Point on the Biscayne aquifer. Simulation results from the high hydraulic conductivity cases indicate the CCS could be having a large effect on the coastal

DOI 10.1007/s10040-009-0502-7

aquifer and that saltwater intrusion may threaten coastal water resources. Conversely, simulations with the low hydraulic conductivity configuration suggest that aquifer salinization is restricted to the immediate vicinity of the CCS and that saltwater intrusion caused by the CCS is limited and not of immediate concern. Future data collection strategies focused on characterizing the current horizontal and vertical extent of saline and thermal plumes at the site and on the aquifer hydraulic properties would help address these issues. For example, recent investigations of the Biscayne aquifer (Cunningham et al. 2009; Renken et al. 2008; Shapiro et al. 2008) demonstrate that relatively thin zones of enhanced porosity are the primary mechanism for lateral solute transport; these and other potentially confounding factors were not investigated here, but would need to be addressed in future work. Furthermore, even though simulated seepage from the CCS is less than maximum plant discharge rates, development of water and salt budgets for the CCS would better constrain aquifer hydraulic properties and aquifer impacts. This information could then be used to help construct and calibrate a three-dimensional transient model of flow and transport that could be used to make a formal assessment and prediction of the impacts of the Turkey Points CCS on groundwater conditions. This three-dimensional representation would also yield a more accurate picture of TDS and thermal transport in regards to instabilities and fingering as two-dimensional models have known limitations in fully representing these important phenomena (Liu and Dane 1997). A formal stability analysis of the CCS system could be used to evaluate the effect of CCS and aquifer parameters on finger plume development and vertical mass transfer rates; results of a stability analysis could be used to further focus data collection activities at the site.

Acknowledgments The authors would like to thank J. D. Decker (US Geological Survey), R. Renken (US Geological Survey), and V. Walsh (Miami-Dade Water and Sewer Department) for reviewing an earlier version of the manuscript. Reviewers for Hydrogeology Journal (E. Abarca, W. E. Sanford, and two anonymous reviewers) provided excellent suggestions that greatly improved the manuscript.

References

Chen F, Chen CF (1993) Double-diffusive fingering convection in a porous medium. Int J Heat Mass Transfer 36(3):793–807

Cunningham KJ, Wacker MA, Robinson E, Dixon JF, Wingard GL (2006) A cyclostratigraphic and borehole-geophysical approach to development of a three-dimensional conceptual hydrogeologic model of the karstic Biscayne aquifer, southeastern Florida. US Geol Surv Sci Invest Rep 2005-5235

Cunningham KJ, Sukop MC, Huang H, Alvarez PF, Curran HA, Renken RA, Dixon JF (2009) Prominence of ichnologically-influenced macroporosity in the karst Biscayne aquifer: stratiform "super-K" zones. Geol Soc Am Bull 121(1–2):164–180

Dames, Moore (1989) Annual report, August 1989, ground-water monitoring program, Turkey Point, Florida, Florida Power and Light Company. Job no. 04598-145-40, Florida Power and Light, Boca Raton, FL

Dausman AM, Langevin CD, Thorne DT Jr., Sukop MC (2009) Application of SEAWAT to select variable-density and viscosity problems. US Geol Surv Sci Invest Rep 2009–5028

Diersch HJG, Kolditz O (1998) Coupled groundwater flow and transport: 2, thermohaline and 3D convection systems. Adv Water Resour 21:401–425. doi:10.1016/S0309-1708(97)00003-1

Fan Y, Duffy CJ, Oliver DS (1997) Density-driven groundwater flow in closed desert basins: field investigation and numerical experiments. J Hydrol 196:139–184

Fish JE (1988) Hydrogeology, aquifer characteristics, and groundwater flow of the surficial aquifer system, Broward County, Florida. US Geol Surv Water Resour Invest Rep 87–4034

Fish JE, Stewart M (1991) Hydrogeology of the surficial aquifer system, Dade County, Florida. US Geol Surv Sci Invest Rep 90–4108

Florida Power and Light (2000) Applicants environmental report: operating license renewal stage Turkey Point units 3 & 4. Florida Power and Light Company Docket Nos. 50–250 and 50–251 revision 1, Florida Power and Light, Boca Raton, FL. http://www.nrc.gov/reactors/operating/licensing/renewal/applications/turkey-point/er.pdf. Cited 28 November 2008

Gaby R, McMahon MP, Mazzotti FJ, Gillies WN, Wilcox JR (1985) Ecology of a population of *Crocodylus acutus* at a power plant site in Florida. J Herpetol 19(2):189–198

German ER (2000) Regional Evaluation of Evapotranspiration in the Everglades. US Geol Surv Sci Invest Rep 00–4217

Guo W, Langevin CD (2002) User's guide to SEAWAT: a computer program for simulation of three-dimensional variable-density ground-water flow. US Geol Surv Tech Water Resour Invest book 6, chap. A7, US Geological Survey, Reston, VA

Griffiths RW (1981) Layered double-diffusive convection in porous media. J Fluid Mech 102:221–248

Harbaugh AW, Banta ER, Hill MC, McDonald MG, (2000) MODFLOW-2000, the U.S. Geological Survey modular ground-water model: user guide to modularization concepts and the ground-water flow process. US Geol Surv Open-File Rep 00-92

Holzbecher E (2005) Groundwater flow pattern in the vicinity of a salt lake. Hydrobiologica 532:233–242

King CW, Holman AS, Webber ME (2008) Thirst for energy. Nat Geosci 1(5):283–286. doi:10.1038/ngeo195

Langevin CD (2001) Simulation of ground-water discharge to Biscayne Bay, Southeastern Florida. US Geol Surv Water Resour Invest Rep 00–4251

Langevin CD (2003) Simulation of submarine ground water discharge to a marine estuary: Biscayne Bay, Florida. Ground Water 41(6):758–771

Langevin CD, Guo W (2006) MODFLOW/MT3DMS-based simulation of variable density ground water flow and transport. Ground Water 44(3):339–351

Langevin CD, Shoemaker WB, Guo W (2003) MODFLOW-2000, the US Geological Survey modular ground-water model: documentation of the SEAWAT-2000 version with the variable-density flow process (VDF) and the integrated MT3DMS transport process (IMT). US Geol Surv Open-File Rep 03–426

Langevin CD, Thorne DT, Dausman AM, Sukop MC, Guo W (2007) SEAWAT Version 4: a computer program for simulation of multi-species solute and heat transport. US Geol Surv Tech Methods, book 6, chap. A22, US Geological Survey, Reston, VA

Langevin CD, Dausman AM, Sukop MC (2009) Solute and heat transport model of the Henry and Hilleke laboratory experiment. Ground Water. doi:10.1111/j.1745-6584.2009.00596.x

Liu HH, Dane JH (1997) A numerical study on gravitational instabilities of dense aqueous phase plumes in three-dimensional porous media. J Hydrol 194:126–142

Lyerly RL (1998) Thermal performance of the Turkey Point cooling canal system in 1998. Report prepared for Florida Power and Light, Miami, FL

Menand T, Woods AW (2005) Dispersion, scale, and time dependence of mixing zones under gravitationally stable and unstable displacements in porous media. Water Resour Res 41, W05014. doi:10.1029/2004WR003701

Nield DA (1968) Onset of thermohaline convection in a porous medium. Water Resour Res 4:553–560
Nield DA, Simmons CT, Kuznetsov AV, Ward JD (2008) On the evolution of salt lakes: episodic convection beneath an evaporating salt lake. Water Resour Res 44, W02439. doi:10.1029/2007WR006161
Noble CV, Drew RW, Slabaugh JD (1996) Soil survey of Dade County area, Florida. Natural Resources Conservation Service, USDA, Washington, DC
Oldenburg CM, Pruess K (1998) Layered thermohaline convection in hypersaline geothermal systems. Transp Porous Media 33:29–63
Oostrom M, Hayworth JS, Dane JH, Güven O (1992) Behavior of dense aqueous phase leachate plumes in homogeneous porous media. Water Resour Res 28(8):2123–2134
Post VEA, Kooi H (2003) Rates of salinization by free convection in high-permeability sediments: insights from numerical modeling and application to the Dutch coastal area. Hydrogeol J 11:549–559. doi:10.1007/s10040-0030927107
Reese RS, Cunningham KJ (2000) Hydrogeology of the Gray Limestone Aquifer in southern Florida. US Geol Surv Sci Invest Rep 99–4213
Renken RA, Cunningham KJ, Shapiro AM, Harvey RW, Zygnerski MR, Metge DW, Wacker MA (2008) Pathogen and chemical transport in the karst limestone of the Biscayne aquifer: 1, revised conceptualization of groundwater flow. Water Resour Res 44(8), W08429. doi:10.1029/2007WR006058
Rubin H (1982) Thermohaline convection in a nonhomogeneous aquifer. J Hydrol 57(3–4):307–320. doi:10.1016/0022-1694(82)90153-6
Rubin H, Roth C (1979) On the growth of instabilities in groundwater due to temperature and salinity gradients. Adv Water Resour 2:69–76. doi:10.1016/0309-1708(79)90013-7
Rubin H, Roth C (1983) Thermohaline convection in flowing groundwater. Adv Water Resour 6:146–156. doi:10.1016/0309-1708(83)90027-1
Sanford WE, Wood WW (2001) Hydrology of coastal sabkhas of Abu Dhabi, United Arab Emirates. Hydrogeol J 9:358–366
Schincariol RA, Schwartz FW (1990) An experimental investigation of variable density flow and mixing in homogeneous and heterogeneous media. Water Resour Res 26(10):2317–2329
Shapiro AM, Renken RA, Harvey RW, Zygnerski MR, Metge DW (2008) Pathogen and chemical transport in the karst limestone of the Biscayne aquifer: 2, chemical retention from diffusion and slow advection. Water Resour Res 44(8), W08430. doi:10.1029/2007WR006059
Shoemaker WB, Cunningham KJ, Kuniansky EL, Dixon J (2008) Effects of turbulence on hydraulic heads and parameter sensitivities in preferential groundwater flow layers. Water Resour Res 44, W03501. doi:10.1029/2007WR006601
Simmons CT, Narayan KA, Wooding RA (1999) On a test case for density-dependent groundwater flow and solute transport models: the salt lake problem. Water Resour Res 35:3607–3620
Simmons CT, Fenstemaker TR, Sharp JM (2001) Variable-density groundwater flow and solute transport in heterogeneous porous media: approaches, resolutions and future challenges. J Contam Hydrol 52:245–275
US Department of Energy (2000) Year 2000 annual steam-electric plant operation and design data. Department of Energy Form EIA-767 data file, USDOE, Washington, DC. http://www.eia.doe.gov/cneaf/electricity/page/eia767hist.html. Cited 25 November 2008
US Department of Energy (2005) Year 2005 annual steam-electric plant operation and design data. Department of Energy Form EIA-767 data file, USDOE, Washington, DC. http://www.eia.doe.gov/cneaf/electricity/page/eia767.html. Cited 25 November 2008
US Nuclear Regulatory Commission (2002) Generic environmental impact statement for license renewal of nuclear plants, Turkey Point Plant, Units 3 and 4. NUREG-1437, supplement 5, US Nuclear Regulatory Commission, Washington, DC. http://www.nrc.gov/reading-rm/doc-collections/nuregs/staff/sr1437/supplement5/index.html. Cited 25 November 2008
Yang X, Dziegielewski B (2007) Water use by thermoelectric power plants in the United States. J Am Water Resour Assoc 43 (1):160–169. doi:10.1111/j.1752-1688.2007.00013.x
Yechieli Y, Wood WW (2002) Hydrogeologic processes in saline systems: playas, sabkhas, and saline lakes. Earth Sci Rev 58:343–365
Zheng C, Wang PP (1999) MT3DMS, a modular three-dimensional multispecies model for simulation of advection, dispersion and chemical reactions of contaminants in groundwater systems: documentation and User's Guide. US Army Engineer Research and Development Center Contract Report SERDP-99-1. USAERDC, Vicksburg, MI